HOKKAIDO UNIVERSITY

Title	Visualization of the entire differentiation process of murine M cells : suppression of their maturation in cecal patches
Author(s)	Kimura, Shunsuke; Yamakami-Kimura, Megumi; Obata, Yuuki; Hase, Koji; Kitamura, Hiroshi; Ohno, Hiroshi; Iwanaga, Toshihiko
Citation	Mucosal immunology, 8(3), 650-660 https://doi.org/10.1038/mi.2014.99
Issue Date	2015-05
Doc URL	http://hdl.handle.net/2115/60152
Type	article (author version)
File Information	manuscript.pdf

Instructions for use

Hokkaido University Collection of Scholarly and Academic Papers : HUSCAP

Title (17/50 words)

Visualization of the entire differentiation process of murine M cells: suppression of their maturation in cecal patches

Running Head (48/50 characters)

Regional differences in M-cell maturation

Authors

Shunsuke Kimura[1,2], Megumi Yamakami-Kimura[1], Yuuki Obata[3,4], Koji Hase[2,4,5], Hiroshi Kitamura[6], Hiroshi Ohno[2,7] and Toshihiko Iwanaga[1]

Affiliations

[1]Laboratory of Histology and Cytology, Graduate School of Medicine, Hokkaido University, North 15, West 7, Kita-ku, Sapporo 060-8638, Japan

[2]Laboratory for Intestinal Ecosystem, RIKEN Center for Integrative Medical Sciences (IMS), 1-7-22 Suehirocho, Tsurumi, Yokohama, Kanagawa 230-0045, Japan

[3]Laboratory for immune regulation, Graduate School of Medicine, Chiba University, Chiba 260-8670, Japan

[4] Division of Mucosal Barriology, The Institute of Medical Science, The University of Tokyo, 4-6-1 Shirokanedai, Minato-ku, Tokyo 108-8639, Japan

[5] PRESTO, Japan Science and Technology Agency, Tokyo 102-0075, Japan

[6]Department of Veterinary Physiology, School of Veterinary Medicine, Rakuno Gakuen

University, Ebetsu, Hokkaido 069-8501, Japan

[7]Division of Immunobiology, Department of Supramolecular Biology, Graduate School of Nanobioscience, Yokohama City University, 1-7-29 Suehiro, Tsurumi, Yokohama 230-0045, Japan

Acknowledgement

We are grateful to Prof. Masahiko Watanabe and Dr. Kohtaro Konno, Laboratory of Anatomy and Embryology, Graduate School of Medicine, Hokkaido University, for their assistance in the production of the polyclonal antibody against Tnfaip2 and the start-up of the FISH analysis. This work was supported by JSPS KAKENHI Grant Numbers 23790521, 25460261 and 24790186. This work was also supported by grants from the Research Foundation for Opto-Science and Technology, and the Mochida Memorial Foundation for Medical and Pharmaceutical Research.

Abbreviations

GP2, Glycoprotein 2; GST, glutathione S-transferase; FISH, fluorescence *in situ* hybridization; DIC, differential interference contrast

Correspondence

Shunsuke Kimura, Ph.D.

Address: North 15, West 7, Kita-ku, Sapporo 060-8638, Japan

Phone and FAX: +81-11-706-7151

E-mail address: skimu@med.hokudai.ac.jp

Disclosures

The authors disclose no conflicts of interests.

Author Contributions

S.K. designed and performed the study, analyzed and interpreted the data, and wrote the manuscript; M.Y.K performed the production of the polyclonal antibody, immunohistochemistry and FISH; Y.O. helped Rag1 KO experiments; H.K., K.H., H.O. and T.I. contributed to the design of the study and revision of the manuscript.

Abstract (180/200)

The microfold (M) cell residing in the follicle-associated epithelium (FAE) is a specialized epithelial cell that initiates mucosal immune responses by sampling luminal antigens. The differentiation process of M cells remains unclear due to limitations of analytical methods. Here we found that M cells were classified into two functionally different subtypes based on the expression of Glycoprotein 2 (GP2) by newly developed image cytometric analysis. GP2-high M cells actively took up luminal microbeads whereas GP2-negative or low cells scarcely ingested them, even though both subsets equally expressed the other M-cell signature genes, suggesting that GP2-high M cells represent functionally mature M cells. Further, the GP2-high mature M cells were abundant in Peyer's patch but sparse in the cecal patch: this was most likely due to a decrease in the nuclear translocation of RelB, a downstream transcription factor for the receptor activator of NF-κB signaling. Given that murine cecum contains a protrusion of beneficial commensals, the restriction of M-cell activity might contribute to preventing the onset of any excessive immune response to the commensals through decelerating the M-cell-dependent uptake of microorganisms.

Introduction

The mucosal surface of the gastrointestinal tract is exposed to a vast array of foreign antigens and microorganisms. The gut-associated lymphoid tissue (GALT) is an important site for inducing mucosal immune responses against potentially hostile exogenous antigens whereas GALT ignores or induces a tolerance to food antigens and commensal microbiota that mainly colonize the distal part of the intestine and establish a mutually beneficial relationship with the host. GALT includes Peyer's patches of the small intestine, their equivalents in the cecum and colon, and isolated lymphoid follicles dispersed throughout the intestine. The dome-shaped follicle-associated epithelium (FAE) covering the luminal surface of lymphoid tissues is characterized by the presence of microfold or membranous epithelial cells, termed M cell.[1] The transcytosis of luminal antigens via M cells is an initial step in the induction of efficient immune responses to certain antigens, such as microorganisms. Although the functions of M cells in mucosal immunity have been noted since their discovery,[2, 3] it is only recently that a molecular basis for the transport of bacteria via M cells has been demonstrated. Glycoprotein 2 (GP2) is expressed on the luminal surface of M cells and interacts with the type I pili of the bacterial outer membrane, consequently mediating the uptake of the type-I-piliated bacteria to initiate subsequent bacteria-specific immune responses.[4] In addition to GP2, several M-cell specific molecules have been identified: Tnfaip2,[5] Pglyrp1,[6] Anxa5,[7] Ccl9,[8] Marksl1,[9] and Spi-B.[10-12] However, comparison of their distribution on the entire FAE has not been analyzed in detail due to limited methods.

Recent studies have also increasingly clarified the molecular basis of M-cell differentiation. The TNF superfamily member receptor activator of NF-κB (RANK) and its ligand (RANKL) are involved in several biological processes. The RANKL-RANK pathway critically regulates the differentiation and/or maturation of M cells.[13] In fact, mice lacking RANKL failed to develop M cells on the Peyer's patch. On the other hand, the administration of RANKL can induce ectopic M cells in the conventional villous epithelium of normal animals,[13] and single Lgr5-positive stem cell can differentiate into M cells in the organoid culture under the presence of RANKL.[10] These effects of the RANKL-RANK pathway on the ectopic M-cell induction are attributed to the up-regulation of the Ets-family transcription factor, Spi-B,[10-12] which is expressed selectively in M cells on FAE. Because Spi-B-deficient mice lack the GP2-expressing M cells in FAE and have a severely reduced capacity for the uptake of luminal antigens, Spi-B is considered to be a major and fundamental regulator of M-cell differentiation.[11] In contrast, Spi-B-deficient mice retain Marksl1- and Anxa5-expressing cells in FAE,[12] which are considered developing M cells. These observations raise the possibility that M-cell precursors may undergo several stages of maturation to differentiate into *bona fide* M cells during the course of their movement along the crypt-FAE dome axis. However, the overall differentiation processes, particularly the regional control of M-cell maturation, have not yet been elucidated.

We here took advantage of a high-resolution immunofluorescent analysis of whole-mount FAE to overview the ontogeny and maturation of M cells. We identified GP2-high M cells as a functional and/or mature subset in Peyer's patches and also

noticed a rare occurrence of GP2-high M cells in the cecal patches. Unlike the Peyer's patch M cells, the majority of cecal patch M cells did not harbor any nuclear RelB that mediates RANKL-RANK signaling. These results suggest that RelB activity has a role in M-cell maturation. This study thus provides a new insight into the regulation of M-cell differentiation.

Results

Identification of two subsets for M cells

To characterize the maturation process of M cells better, we developed a new method to perform immunostaining and FISH of freshly isolated FAE monolayers, including the FAE-associated crypt (Supplemental Figure 1). The obtained specimens were exclusively composed of epithelial monolayers and were not accompanied by any serious changes on the localization of the junctional proteins, ZO-1 and E-cadherin (Supplemental Figure 1d), indicating that the integrity was well maintained after treatment with EDTA.

We first applied this specimen to a whole-mount immunohistochemical staining of representative M-cell markers, Tnfaip2 and GP2,[4, 5] to detect the M cell lineage. The immunostaining for these markers visualized cells arranged in radial stripes on the crypt-FAE axis (Figure 1a). Numerous cells expressing Tnfaip2 but not GP2 had already appeared in the orifice of crypts while cells expressing both Tnfaip2 and GP2 were present from the middle to the top of the FAE dome (Figure 1a, b). Confocal microscopy combined with F-actin staining revealed that, irrespective of the GP2 expression level, Tnfaip2-expressing cells have characteristic morphological features of typical M cells, namely an irregular brush border and basolateral pocket embracing lymphocytes (Supplemental Figure 2).[1] These features were also confirmed by immunoelectron-microscopic analysis (Supplemental Figure 3). The α1-2 fucose-specific lectin *Ulex europaeus* agglutinin I (UEA-I), which is a classical M-cell

marker of the mouse Peyer's patch,[14] recognized Tnfaip2-expressing cells (Supplemental Figure 4). These data revealed that M cells homogeneously express Tnfaip2 whereas the GP2 expression level differed among M cells. To quantitate their proportion, we measured fluorescence intensities of immunoreactivities for Tnfaip2 and GP2 in individual M cells (Figure 1c). The scatter plot revealed that M cells could be divided into two subsets by the intensity of the GP2 expression, namely, GP2-high ($GP2^{high}$) and GP2-negative or low ($GP2^{-/low}$) M cells (Figure 1d).

GP2-high M cells predominantly take up luminal antigens

Whole-mount immunohistochemistry combined with EdU-pulse labeling revealed that Gp2-expressing cells were appeared at a later stage than Tnfaip2-expressing cells (Supplemental Figure 5). Since GP2 is an antigen-uptake receptor on M cells,[4] we considered that the $GP2^{high}$ M cells may be functionally matured M cells. To confirm this idea, we examined the uptake capacity of the M-cell subsets by a ligated intestinal loop assay using 20 nm fluorescent latex beads. The beads appeared densely within $GP2^{high}$ M cells but only occasionally in $GP2^{-/low}$ M cells (Figure 2a). We noted that the beads were located internally in $GP2^{high}$ M cells under our experimental conditions (Figure 2b). Furthermore, the image analysis of fluorescence intensities of beads in M cells demonstrated that strong signals were detected on the $GP2^{high}$ M cells while intermediate or no signals were found in the $GP2^{-/low}$ cells (Figure 2c). These data indicate that the GP2-high subset serves as active or mature M cells with a high uptake capacity of luminal antigens.

M cells express a set of fundamental genes including Spib

We subsequently performed a multicolor FISH analysis on the FAE sheets to characterize the gene expression profiles of the two M-cell subsets (Figure 3). The FISH analysis confirmed the existence of *Gp2*-negative or low and *Gp2*-high M-cell subsets (Figure 3b), in agreement with the results from the whole-mount immunohistochemistry. *Spib* is an essential transcription factor for M-cell differentiation.[10-12] The expression of *Spib* was detected continuously from the crypts to the top of the FAE dome (Figure 3a). Image analysis showed that the expression level of *Spib* was indistinguishable between both subsets (Figure 3c). The distributions of the three marker genes were further confirmed at the protein level by immunohistochemistry (Supplemental Figure 6). Pulse chase experiments with EdU labeling revealed that Spi-B is expressed from the earliest stage among the three M-cell markers (Supplemental Figure 5), confirming that Spi-B is indeed extant early on in M-cell differentiation.

We further examined the distribution of three other M cell marker genes: *Pglyrp1*,[6] *Anxa5*,[7] and *Ccl9*,[8] with *Spib* and *Gp2* serving as indexes of M-cell differentiation levels. These were expressed in both $Gp2^{-/low}$ and $Gp2^{high}$ M-cell subsets, and their distribution on the crypt-FAE axis was similar to that of *Spib* (Supplemental Figure 7). Thus, *Spib*, *Pglyrp1*, *Anxa5*, and *Ccl9* were considered fundamental signature genes of M cells simultaneously expressed prior to *Gp2* expression.

M cell maturation is suppressed in the cecal FAE

We made an immunohistochemical comparison of the proportions of GP2-high M cells among organized lymphoid follicles from the duodenum, ileum, cecum, and colon in BALB/c or C57BL/6 mice (Figure 4a). It is worth noting that the number and proportion of $GP2^{high}$ M cells were both significantly lower in the FAE of cecal patches; in particular, they were rarely found in C57BL/6 mice (Figure 4a and Supplemental Figure 8). The cecal M cells in C57BL/6 mice consist almost entirely of $GP2^{-/low}$ cells with a low uptake capacity of luminal microbeads. The GP2-high subset in cecal patches of BALB/c mice has a higher uptake capacity similar to that in Peyer's patches (Figure 4b-c). Whole-mount FISH analysis also demonstrated that *Gp2* expression was not detectable in the FAE of cecal patches from C57BL/6 mice whereas *Spib* and *Tnfaip2* expression were detectable (Supplemental Figure 8). The cecal M cells also intensely expressed other signature genes: *Pglyrp1*, *Anxa5,* and *Ccl9*. These findings imply that the cecal FAE constructs a M-cell lineage; however, their activation or maturation is suppressed.

It is well known that the interaction of FAE cells with B lymphocytes, some pathogenic bacteria, and luminal microbial environment influence M-cell differentiation.[1] FAE-derived CCL20 attracts CCR6-positive B lymphocytes toward the FAE, and in turn, the association with B cells in close proximity facilitates M-cell differentiation in the FAE.[15, 16] We therefore examined whether the arrest of M-cell maturation in the cecal patches can be attributed to the down-regulation of CCL20 (Supplemental Figure 9a). The distribution and expression of CCL20 in the cecal FAE did not differ from those in the ileal FAE. Moreover, RAG1-deficient mice[17]--which

lack mature B and T cells--showed equivalent proportions of GP2-high M cells with control mice (50.76 ± 11.87 % in Rag1-KO mice and 59.73 ± 12.19 % in control C57BL/6 mice). These data suggest that the association of B cells with FAE is not a cause of the arrest of M cell maturation. When we measured the proportion of GP2-positive cells in germ free mice, their populations were also identical with those of conventional mice (Supplemental Table 3). Notwithstanding the fact that some pathogenic bacteria could induce the transition of enterocytes to M cells,[18] commensal microorganisms appear to contribute little to induction of M-cell differentiation.

RANKL-RANK signaling is necessary but insufficient for maturation into GP2-high M cells

RANKL-RANK signaling is indispensable for the initiation of M-cell differentiation in Peyer's patches.[13] We therefore investigated expressions of RANKL and RANK in the cecal patches. Immunohistochemical analysis showed that subepithelial stromal cells intensely expressed RANKL in the cecal patches, and RANK was expressed throughout the cecal epithelium (Supplemental Figure 9b). The distributions of these molecules were essentially identical to those in Peyer's patches.[13] Exogenouse RANKL has been used to induce ectopic M cells experimentally in the villus region.[11, 13] We also confirmed that administrations of the GST-RANKL fusion protein markedly increased the proportion of GP2-high cells in the ileal FAE. However, the GST-RANKL treatment failed to increase the proportion of GP2-high M cells in cecal FAE (Figure 5a, b). Of note, immature ($GP2^{-/low}$ $Tnfaip2^{+}$) M cells were augmented by this treatment as

observed in Peyer's patches (Figure 5a, c). Likewise, exogenous GST-RANKL treatment ectopically induced GP2-high M cells in the conventional epithelium of the ileum but not in the cecum of C57BL/6 mice, where most M cells were of the immature type (Figure 5d). Our quantitative PCR analysis further confirmed that the administration of GST-RANKL up-regulated the expressions of *Spib* and *Tnfaip2* but not *Gp2,* in the cecal epithelium of C57BL/6 mice (Figure 5e). The induction of *Gp2* expression in the cecal epithelium was detectable in BALB/c mice but was also suppressed as compared with that in the ileal epithelium. These findings illustrated that the RANKL-RANK signaling is necessary for a lineage commitment to M cells but is insufficient for full maturation into GP2-high M cells in the cecal patches.

Lower RelB activity contributes to the inhibition of M-cell maturation in the cecal FAE

RelB, a member of the NF-κB family, is essential for the RANKL-induced cellular differentiation of osteoclasts.[19] RelB is retained in the cytoplasm as latent inactive form, until it is activated and rapidly transported into the nucleus.[20] We examined the RelB activity during M-cell differentiation in ectopic RANKL-induced M cells (Figure 6a). Nuclear translocation of RelB could be confirmed one day after RANKL administration in both ileal and cecal epithelium, and the amount of nuclear RelB was lower in the cecal epithelium than in the ileal one. On the other hand, we failed to find any change in the amount of nuclear RelA/p65 after RANKL administration, which is another member of the NF-κB family.[20] The decrease in RelB

nuclear translocation in the cecum raised a possibility that RelB activity may be associated with full maturation and/or development of M cells. To examine this possibility, we used alymphoplasia *(aly/aly*) mice which have a point mutation in *Map3k14* gene causing loss of function of the NF-κB inducing kinase,[21] and accordingly RelB failed to move into nuclei.[19] Because the *aly/aly* mice lack secondary lymphoid organs--including Peyer's patches,[22] we carried out our analysis by ectopic induction of M cells in intestinal epithelium after GST-RANKL administration (Figure 6b). The result was that both $GP2^{high}$ and $GP2^{-/low}$ M cells were not induced in *aly/aly* mice, indicating that RelB nuclear translocation is essential for the formation of M cells.

To clarify the role of RelB on the regional differences in M-cell maturation, we performed whole-mount immunohistochemistry using anti-Spi-B antibodies followed by Hoechst 33342 to detect nuclei (Figure 7). The proportion of cells expressing nuclear RelB was significantly smaller in cecal FAE than in ileal FAE, regardless of mouse strains (Figure 8a and c). Moreover, RelB-positive M cell populations were significantly lower in cecal patches than in Peyer's patches (Figure 8 b and c). This was particularly evident in the C57BL/6 mice (Figure 8c); the RelB-positive M cell population occupied 93.1 ± 1.7% of M cells in the ileal FAE of C57BL/6 mice while this population accounted for only 42.5 ± 1.3% in the cecal FAE ($P < .001$). RelB-positive cells were found in the crypt and RelB-negative cells appeared in the FAE (Figure 7b), indicating that RelB activity is maintained at the initiation of their differentiation and then down-regulated in the cecal FAE of C57BL/6 mice.

Discussion

In this study, we newly identified two distinct M cell subsets on the basis of the expression level of GP2, namely, $GP2^{high}$ and $GP2^{-/low}$ M cells. These subsets not only possessed the UEA-I-labeling property as well as similar expression levels of other M-cell signature genes including Spi-B, but also shared morphological features characteristic for M cells. Nevertheless, the GP2-high subset had a higher capacity for taking up luminal microbeads, indicating that this subset comprises functionally mature M cells. The molecular mechanisms of M cell differentiation and maturation are still largely unknown. Spi-B has been well documented as an essential transcription factor for regulating the differentiation of immature M cells into functionally mature M cells in Peyer's patches.[1, 10-12, 16] That said, our data challenged this idea because fully matured M cells were not generated in the cecum, even in the presence of Spi-B. Recent transcriptome analyses have revealed that several M-cell-specific genes including *Gp2*, *Tnfaip2*, and *Ccl9* were down-regulated in Spi-B KO mice.[11] However, the expression of other M-cell specific genes including *Pgryrp1* and *Anxa5* was not affected by the lack of Spi-B,[12] and the forced expression of Spi-B in an *in vitro* organoid culture was insufficient to induce M-cell differentiation.[10] Taking our data and the previous studies into account, we consider that Spi-B is essential for the initiation of M-cell differentiation and, in addition to Spi-B, other regulator(s) may be required for controlling the definite differentiation into the mature GP2-high M cells.

Exogenous RANKL administration into mice could induce ectopic M-cell differentiation in intestinal epithelium.[13] On this occasion, we found that RelB was

transported into the nucleus in the conventional epithelium immediately after RANKL administration. RelB is the non-canonical NF-κB transcription factor essential for RANKL-mediated cellular differentiation in several cell types.[19, 20] This transcription factor is originally produced in the cytoplasm and, upon activation, transported to the nucleus where it transactivates target genes. The RelB translocation is dependent on NF-κB inducing kinase (NIK) activity.[19] It is well known that RelB-deficient mice and NIK mutant (*aly/aly*) mice in which RelB failed to move into nuclei are devoid of secondary lymphoid organs, including GALTs.[22, 23] By using *aly/aly* mutant mice with ectopic induction of M cells after RANKL administration, we demonstrated that the nuclear translocation of RelB is essential for the M-cell differentiation. The quantitative image analysis in C57BL/6 mice also demonstrated that, in contrast to the ileal M cells expressing nuclear RelB, a major population of cecal M cells of C57BL/6 mice did not express nuclear RelB and remained GP2-negative or low immature M cells. In the BALB/c mice, maturation of M cells into GP2-high cells occurred with much higher frequency. Correspondingly, the proportion of RelB-positive M cells was higher in cecal patches of BALB/c mice than those of C57BL/6 mice. That is, the RelB activity in M cells was correlated with the degree of their maturation. Our data suggest that RelB is required for the initiation of M-cell differentiation and also is a key determinant of their maturation by regulating the induction of some downstream genes.

Several groups have mentioned the different phases of M-cell differentiation, as shown by their glycoconjugate profiles and morphological features;[24-26] however, they lack the evidence which shows the relationship between the M-cell function and its

gene expression. Our study gives a new and more reliable way to visualize their differentiation process using the M-cell specific molecular markers. In fact, by analyzing the proportion of GP2-high M cells, we found that M-cell maturation level differs among GALTs located at different regions as well as mouse strains. Notably, $GP2^{high}$ M cells were scarce in the cecal patches of C57BL/6 mice while $GP2^{-/low}$ M cells were predominant there, and uptake of luminal microbeads by cecal M cells in C57BL/6 mice was hardly observed. In BALB/c mice, the proportion of $GP2^{high}$ M cells in the cecal patches was approximately 50%, which was much higher than that of C57BL/6 mice (approximately 1%) but still lowest among the GALTs of BALB/c mice. The induction of ectopic $GP2^{high}$ M cells by GST-RANKL treatment was also suppressed in the cecal FAE of BALB/c mice. These data revealed that the M-cell maturation process is commonly suppressed in the cecum in both strains. As mentioned above, the suppression of M-cell differentiation was most likely due to a decrease in the nuclear translocation of RelB. It is considered that subepithelial lymphocytes and luminal bacteria impact on the M-cell differentiation.[1] Our study, however, showed that the proportion of $GP2^{high}$ M cells is largely unaltered in Rag1-deficient mice and germ free mice. Thus, the suppression of M-cell differentiation in cecal patches might be controlled by cell intrinsic pathway, rather than due to the extrinsic factors.

The present study demonstrated the regional differences in M-cell maturation regulated by RelB activity. Cecal patches have adequate ability to induce antigen-specific immunoglobulin responses as with Peyer's patchs and generate IgA-secreting cells migrating to the large intestine.[27] Huge number of commensal

bacteria inhabit in the cecum, because the cecum in the mouse is a major site for microbial fermentation. Given that the M-cell-dependent antigen uptake initiates an antigen-specific mucosal immune response, it is possible to speculate that the attenuated M-cell maturation may prevent excess antigen uptake and subsequent immune response and therefore contribute to establish a mutualistic symbiosis with commensal microbiota abundantly colonizing in the cecum of mice. Further experimental evidence will be required to determine this conclusively.

Methods

Animals

BALB/cCrSlc (BALB/c) and C57BL/6NCrSlc (C57BL/6) mice 7-12 weeks old were obtained from Japan SLC (Hamamatsu, Japan) and maintained under conventional conditions. BALB/cCrSlc and C57BL/6NCrSlc germ free mice 7 weeks old were also purchased from Japan SLC. RAG-1 null mice (C57BL/6 background) were purchased from The Jackson Laboratory (Bar Harbor, ME, USA). ALY/NscJcl-aly/aly and ALY/NscJcl-aly/+ mice 8-10 weeks old were purchased from CLEA Japan, Inc. (Osaka, Japan). All animals were treated according to the laboratory animal control guidelines of Hokkaido University (Approval #13-0052) which conform to the Guide for the Care and Use of Laboratory Animals of the U.S. Institute for Laboratory Animal Research.

Production of polyclonal antibody against Tnfaip2

A polyclonal antibody was raised against amino acid residues 40-691 of mouse Tnfaip2 (also known as M-Sec; NP_033422) in a rabbit. The polypeptides were expressed as glutathione S-transferase (GST) fusion proteins in *Escherichia coli* strain BL21 (DE3) (Life Technologies, Grand Island, NY, USA) by addition of 0.1 mM isopropyl-β-D-thiogalactopyranoside (IPTG) for 16 hours at 25°C. The fusion protein was purified with glutathione-Sepharose 4B (GE Healthcare, Waukesha, WI, USA), and GST was removed by on-column cleavage with thrombin protease. Resulted poypeptide was emulsified with Freund's complete adjuvant (Difco, Detroit, MI, USA), and injected subcutaneously into female New Zealand White rabbits six times every other

week. Two weeks after the sixth injection, affinity-purified antibodies were prepared using antigen coupled to cyanogens bromide-activated Sepharose 4B (GE Healthcare). The specificity of the antibody was confirmed by Western blotting and immunohistochemistry of tissues from Tnfaip2 knockout mice.

Preparation of FAE and conventional epithelial monolayers

FAE was isolated from mouse Peyer's patches and cecal patches by modifying the method described by Hase et al.[8] Briefly, Peyer's patches and cecal patches were soaked in ice-cold Hank's balanced salt solution (Life Technologies) containing 30 mM EDTA and 5 mM dithiothreitol. After incubation with gentle shaking for 20 min on ice, FAE monolayers containing both dome and crypt regions were carefully separated from lymphoid follicles by manipulation with a fine needle under stereomicroscopic monitoring. Conventional epithelial monolayers were also isolated in the same manner from small pieces of the ileum and cecum.

Immunohistochemistry

For whole-mount staining, the isolated epithelium was fixed with 4% paraformaldehyde (PFA) in PBS for 30 min. For conventional observation, frozen sections 10 μm in thickness were mounted on poly-L-lysine-coated glass slides, air-dried, and fixed with 4% PFA in PBS for 30 min. After preincubation with 10% normal donkey serum for 1 hour, the specimens were incubated with primary antibodies (Supplemental Table 1) or *Ulex europaeus* agglutinin I (UEA-I) lectin (Vector laboratories, Barlingame, CA, USA)

in the presence of 0.2% saponin and 0.2% bovine serum albumin in PBS overnight at 4˚C, followed by incubation with appropriate secondary antibodies for 2 hours at room temperature. For detecting filamentous actin, we used fluorescently-labeled phalloidin (Acti-Stain 670 diluted at 1:400, Cytoskeleton, Inc., Denver, CO, USA) along with the primary antibodies. For nuclear staining, we used 4', 6-diamidino-2-phenylindole, dihydrochloride (DAPI), TOPRO-3 or Hoechst 33342 (Life Technologies) after incubation with the secondary antibodies. The specimens were observed using a confocal laser microscope FV300 or FV1000 (Olympus, Tokyo, Japan) after mounting with SlowFade Gold antifade reagent (Life Technologies).

For immunoelectron microscopy, PFA-fixed Peyer's patches were processed for the preembedding silver-intensified immunogold method. Frozen sections were incubated with anti-Tnfaip2 and subsequently reacted with goat anti-rabbit IgG covalently linked to 1.4 nm gold particles (BBinternational, Cardiff, UK). After silver enhancement (HQ silver, Nanoprobes, NY, USA), sections were osmificated, dehydrated, and embedded in Quetol 812. Ultrathin sections were prepared and stained with uranyl acetate and lead citrate for observation under a transmission electron microscope (H-7100, Hitachi, Tokyo, Japan).

Fluorescent *in situ* hybridization (FISH)

FISH was performed using the Quantigene View RNA ISH Cell Assay (Affymetrix, Santa Clara, CA, USA) with slight modifications in the fixation and the protease digestion steps. Briefly, isolated epithelium was fixed in a solution containing 4% PFA

and 0.5% glutaraldehyde in PBS for 3 hours on ice and then transferred to 4% PFA in PBS, followed by overnight incubation at 4˚C. After three washing with 50 mM glycine in PBS, the specimens were pretreated with a detergent solution (Affymetrix) for 10 min and then protease QS (dilution 1:400 in PBS; Affymetrix) or 0.1 mg/ml proteinase K in PBS (Kanto Chemical co., inc., Tokyo, Japan) for 10 min at room temperature. The following processes were in accordance with the manufacturer's protocol. Specific oligonucleotide probe sets against *Gp2* (catalog No. VB6-13947), *Tnfaip2* (VB4-13531), *Spib* (VB1-13735 and VB4-13734), *Pglyrp1* (VB1-14469), *Anxa5* (VB1-13956), and *Ccl9* (VB1-13952) were purchased from Affymetryx, Inc.

Ligated intestinal loop assay

To prepare ligated intestinal loops, the mice were anesthetized using a halothane vaporizer. Aliquots of 1×10^{11} fluorescent polystyrene latex beads (20 nm diameter; Life Technologies) were injected into the ligated intestinal loop as described previously.[4] The mice were euthanized 30 min after the injection, and FAE monolayers were isolated as described above.

Image analysis

Confocal images were acquired in the photon counting mode of a FV1000 confocal microscopy system with FV10-ASW software (Olympus). To calculate the population of GP2-high cells, we selected the region of M cells by setting a threshold of signal intensities for GP2 and/or Tnfaip2 and then calculated mean fluorescence intensities

within these regions by using ImageJ software.[28] Obtained values were plotted by Microsoft Excel software or saved as converted from a comma-separated values (csv) format to a flow cytometry standard (fcs) format using a CsvToFcs module of GenePattern software.[29] The fcs files were opened and analyzed by FlowJo software (TreeStar Inc., Ashland, OR, USA). In the case of Figure 6, we selected the region of nuclei by setting threshold of signal intensities for Hoechst 33342 and measured the nuclear fluorescence intensities of Spi-B and RelB.

Pulse-chase experiments

Mice were administered with 5-ethynyl-2'-deoxyuridine (EdU, 5mg/kg of body weight) by intraperitoneal injection. EdU detection was carried out using the Click-iT EdU AlexaFluor488 imaging kit (Life Technologies) according to the manufacture's protocol.

RANKL administration

The primers 5′-CACCCCCGGGCAGCGCTTCTCAGGAGCT-3′ and 5′-GAGACTCGAGTCAGTCTATGTCCTGAAC-3′ (Sigma Genosys Inc., Woodlands, Texas, USA) were used for a polymerase chain reaction (PCR) to amplify a cDNA clone of RANKL. The PCR fragment was subcloned into the pGEX-4T-2 vector (GE Healthcare) after digestion by *SmaI* and *XhoI*. The construct was transformed into the BL21 *Escherichia coli* strain for glutathione-S-transferase (GST) fusion protein expression. The culture was induced with 0.1 mM isopropyl

β-D-1-thiogalactopyranoside for 16 hours at 20˚C, and the GST-RANKL was purified from bacterial lysate by affinity chromatography on a Glutathione-Sepharose 4B (GE Healthcare) followed by dialysis against multiple changes of PBS. Recombinant GST used as a control was prepared by the same method using an empty pGEX-4T-2 vector. Purified protein was administered to mice by intraperitoneal injections of 250 μg per day for three days, according to a previous report with minor modification.[13] After 24 hours from the last administration, the mice were sacrificed and subjected to the following assays.

Quantitative reverse transcriptase PCR (RT-PCR)

Total RNA was prepared using TRIzol (Life Technologies) from isolated epithelium from mice injected with GST or GST-RANKL. First-strand cDNA synthesis was completed using ReverTra Ace (TOYOBO, Osaka, Japan). Quantitative PCR reactions were conducted in Rotor Gene 6000 equipment (Qiagen, Hilden, Germany) using KAPA SYBR Green Fast PCR kit (KAPA Biosystems, Woburn, MA, USA). The specific primers used are shown in Supplemental Table 2.

Western Blotting

The small pieces of isolated epithelial sheets (about 30 mm length) from GST-RANKL injected mice intestine were washed with ice-cold HBSS and suspended in 0.5 ml of lysis buffer [10 mM Hepes-NaOH pH7.9, 1.5 mM $MgCl_2$, 10 mM KCl, 0.1 mM EDTA, 1 mM dithiothreitol (DTT), 0.1% NP-40, protease inhibitor cocktails (Roche,

Mannheim, Germany)]. The epithelial sheets were allowed to swell on ice for 15 min, and then vortexed vigorously for 15 s. The homogenate was centrifuged at 850 g for 10 min. The supernatant (postnuclear extract) were added 6x SDS sample buffer and stored at -30˚C. The resulted pellet was washed with 0.5 mL lysis buffer and centrifuged with same condition, and then re-suspended 50 μL in ice-cold nuclear extraction buffer [20 mM Hepes-NaOH pH7.9, 1.5 mM MgCl2, 400 mM NaCl, 0.1 mM EDTA, 0.1% NP-40, 10 % glycerol, 10 mM DTT, protease inhibitor cocktail (Roche)], and incubated on ice for 30 min with intermittent mixing. Samples were centrifuged at 14,000 g for 30 min, and the supernatant (nuclear extract) was added 6x SDS sample buffer and stored at −30˚C. Equal amounts of post-nuclear and nuclear extract were separated on 12% polyacrylamide gels and transferred to PVDF membrane. Standard immunostaining was carried out using ECL enhanced chemiluminescence technique (GE Healthcare). The primary antibodies used for western blotting were shown in Supplemental Table 1.

Statistical analysis

Differences between the two groups were analyzed by Student's *t*-test. Differences for multiple group comparisons were analyzed by a one-way analysis of variance (ANOVA) followed by Dunnett's test. All statistical analyses were conducted using R software (http://www.r-proj- ect.org/).

Disclosures

The authors disclose no conflicts of interests.

References

1. Mabbott N.A., Donaldson D.S., Ohno H, Williams, I.R. & Mahajan, A. Microfold (M) cells: important immunosurveillance posts in the intestinal epithelium. *Mucosal Immunol* **6**:666-77 (2013).
2. Bockman D.E. & Cooper M.D. Pinocytosis by epithelium associated with lymphoid follicles in the bursa of Fabricius, appendix, and Peyer's patches. An electron microscopic study. *Am J Anat* **136**:455-77 (1973).
3. Owen R.L. & Jones A.L. Epithelial cell specialization within human Peyer's patches: an ultrastructural study of intestinal lymphoid follicles. *Gastroenterology* **66**:189-203 (1974).
4. Hase K., *et al.* Uptake through glycoprotein 2 of FimH(+) bacteria by M cells initiates mucosal immune response. *Nature* **462**:226-30(2009).
5. Hase K., *et al.* M-Sec promotes membrane nanotube formation by interacting with Ral and the exocyst complex. *Nat Cell Biol* **11**:1427-32 (2009).
6. Lo D., *et al.* Peptidoglycan recognition protein expression in mouse Peyer's Patch follicle associated epithelium suggests functional specialization. *Cell Immunol* **224**:8-16 (2003).
7. Verbrugghe P., Waelput W., Dieriks B., Waeytens, A., Vandesompele, J. & Cuvelier, C. A. Murine M cells express annexin V specifically. *J Pathol* **209**:240-9 (2006).
8. Hase K., *et al.* Distinct gene expression profiles characterize cellular phenotypes of follicle-associated epithelium and M cells. *DNA Res* **12**:127-37 (2005).
9. Terahara K., *et al*. Comprehensive gene expression profiling of Peyer's patch M cells, villous M-like cells, and intestinal epithelial cells. *J Immunol* **180**:7840-6 (2008).
10. de Lau W., *et al.* Peyer's patch M cells derived from Lgr5(+) stem cells require SpiB and are induced by RankL in cultured "miniguts". *Mol Cell Biol* **32**:3639-47 (2012).
11. Kanaya T., et al. The Ets transcription factor Spi-B is essential for the differentiation of intestinal microfold cells. *Nat Immunol* **13**:729-36 (2012).
12. Sato S., *et al*. Transcription factor Spi-B-dependent and -independent pathways

for the development of Peyer's patch M cells. *Mucosal Immunol* **6**:838-46 (2013).

13. Knoop K.A., *et al*. RANKL is necessary and sufficient to initiate development of antigen-sampling M cells in the intestinal epithelium. *J Immunol* **183**:5738-47 (2009).
14. Clark M.A., Jepson M.A., Simmons N.L, Booth T.A. & Hirst, B.H. Differential expression of lectin-binding sites defines mouse intestinal M-cells. *J Histochem Cytochem* **41**:1679-87 (1993).
15. Lugering A., *et al.* Absence of CCR6 inhibits CD4+ regulatory T-cell development and M-cell formation inside Peyer's patches. *Am J Pathol* **166**:1647-54 (2005).
16. Kobayashi A., *et al*. The functional maturation of M cells is dramatically reduced in the Peyer's patches of aged mice. *Mucosal Immunol* **6**:1027-37 (2013).
17. Mombaerts P., Iacomini J., Johnson R.S., Herrup, K., Tonegawa. S. & Papaioannou, V.E. RAG-1-deficient mice have no mature B and T lymphocytes. *Cell* **68**:869-77 (1992).
18. Tahoun A., *et al*. Salmonella transforms follicle-associated epithelial cells into M cells to promote intestinal invasion. *Cell Host Microbe* **12**:645-56 (2012).
19. Vaira S., *et al*. RelB is the NF-kappaB subunit downstream of NIK responsible for osteoclast differentiation. *Proc Natl Acad Sci U S A* **105**:3897-902 (2008).
20. Shih V.F., Tsui R., Caldwell A. & Hoffmann, A. A single NFkappaB system for both canonical and non-canonical signaling. *Cell Res* **21**:86-102 (2011).
21. Shinkura R., *et al*. Alymphoplasia is caused by a point mutation in the mouse gene encoding Nf-kappa b-inducing kinase. *Nat Genet* **22**:74-7 (1999).
22. Miyawaki S., *et al*. A new mutation, aly, that induces a generalized lack of lymph nodes accompanied by immunodeficiency in mice. *Eur J Immunol* **24**:429-34 (1994).
23. Yilmaz Z.B., Weih D.S., Sivakumar V. & Weih, F. RelB is required for Peyer's patch development: differential regulation of p52-RelB by lymphotoxin and TNF. *EMBO J* **22**:121-30 (2003).
24. Bye W.A., Allan C.H. & Trier JS. Structure, distribution, and origin of M cells in Peyer's patches of mouse ileum. *Gastroenterology* **86**:789-801 (1984).

25. Gebert A., Fassbender S., Werner K. & Weissferdt, A. The development of M cells in Peyer's patches is restricted to specialized dome-associated crypts. *Am J Pathol* **154**:1573-82 (1999).
26. Lelouard H., Sahuquet A., Reggio H. & Montcourrier, P. Rabbit M cells and dome enterocytes are distinct cell lineages. *J Cell Sci* **114**:2077-83 (2001).
27. Masahata K., *et al*. Generation of colonic IgA-secreting cells in the caecal patch. *Nat Commun* **5**:3704 (2014).
28. Schneider C.A., Rasband W.S. & Eliceiri K.W. NIH Image to ImageJ: 25 years of image analysis. *Nat Methods* **9**:671-5 (2012).
29. Reich M, Liefeld T, Gould J., Lerner, J. Tamayo, P. & Mesirov, J. P. GenePattern 2.0. *Nat Genet* **38**:500-1 (2006).

Figure Legends

Figure 1

GP2 expression defines two M-cell subsets.

(**a**) A confocal image of a whole-mount immunostaining of the isolated FAE monolayer from an ileal Peyer's patch of a BALB/c mouse for Tnfaip2 (Green) and GP2 (Magenta). (**b**) An enlarged view of the squared area in panel a. (**c**) Histograms of fluorescence intensity obtained from the confocal images. The x-axis represents fluorescence intensity in arbitrary units on a log10 scale, and the y-axis is the number of cells found at each fluorescence level (normalized to mode). Red lines represent cells stained with either the anti-Tnfaip2 or GP2 antibody. Gray lines show background fluorescence intensities obtained from control experiments without primary antibodies. (**d**) Scatter plot of the fluorescence intensities of Tnfaip2 versus GP2, where each dot represents a single cell. The capital N indicates the number of analyzed cells. The proportions of cells within the indicated boxed areas were calculated by FlowJo software as described in *Methods*. Scale bars: 200 μm (a) and 50 μm (b).

Figure 2

$GP2^{high}$ M cells have a high uptake capacity of luminal latex beads.

(**a**) Confocal images of whole-mount immunostaining of the ileal FAE for Tnfaip2 (Green) and GP2 (Cyan). Latex beads (Magenta) were injected into the ligated

intestinal loop of a BALB/c mouse as described in Methods. (**b**) High magnification image of M cells taking up latex beads (upper panels) and a sliced image (lower panels) reconstructed from consecutive confocal microscope images. (**c**) Scatter plots of the fluorescence intensities of Tnfaip2 versus GP2 (the upper panel). The lower panel shows histograms of the fluorescence intensity of latex beads in $GP2^{high}$ (Red line) or $GP2^{-/low}$ (Blue line) M cells within the indicated boxed areas of the scatter plot. Scale bars: 20 μm (a) and 10 μm (b).

Figure 3

Spib is expressed in the earliest stage of M-cell differentiation and shared by $Gp2^{high}$ and $Gp2^{-/low}$ M cells.

(**a**) Three-color FISH image of the ileal FAE from a BALB/c mouse with oligonucleotide probes for *Spib*, *Tnfaip2*, and *Gp2*. Each indicated channel is shown separately in the gray scale. DIC: differential interference contrast. (**b**) Scatter plots comparing signal intensities of *Gp2* and *Tnfaip2*. (**c**) The histogram of the fluorescence intensity of *Spib* in $Gp2^{high}$ (Red) or $Gp2^{-/low}$ (Blue) M cells within the indicated boxed areas of the scatter plot. A gray line shows background fluorescence intensities obtained from control experiments without specific oligonucleotide probes. Scale bars: 100 μm (a).

Figure 4

Suppression of M-cell maturation in cecal patches.

(**a**) Scatter plot summarizing the proportions of $GP2^{high}$ cells of GALT obtained from BALB/c (the upper panel) and C57BL/6 (the lower panel) strains. The proportions were calculated by using FlowJo software as shown in Figure 1. Each dot represents individual FAE, and horizontal bars indicate median values. The results are based on three to six mice. Colonic patches could not be detected in the colon of C57BL/6 mice. ***$P < .001$; P values were calculated by Dunnett's test. (**b** and **c**) Scatter plots of the fluorescence intensities of Tnfaip2 versus GP2 (the left panels). The right panels show histograms of the fluorescence intensity of latex beads in $GP2^{high}$ (solid lines) or $GP2^{-/high}$ (dashed lines) M cells within the indicated boxed areas of the scatter plot.

Figure 5

Administration of RANKL fails to induce the development of $GP2^{high}$ M cells in the cecum.

(**a**) Whole-mount immunohistochemical images of Tnfaip2 and GP2 in ileal and cecal FAEs. Left panels are the FAEs from C57BL/6 mice administrated with GST (control), and right panels are those with GST-RANKL. Administrations of GST or GST-RANKL were performed as described in *Methods*. (**b** and **c**) The left panels show scatter plots summarizing the proportions of $GP2^{high}$ M cells (b). The right panels show scatter plots summarizing the frequency of Tnfaip2-positive M cells in individual FAE from the indicated lymphoid organs(c). **$P < .05$, ***$P < .001$; P values were calculated by Dunnett's test. (**d**) Whole-mount immunohistochemical images of Tnfaip2 and GP2 in conventional epithelia from the ileum and cecum of GST (control)

or GST-RANKL injected C57BL/6 mice. The ileal specimen is composed of three villi and many crypts. (**e**) Quantitative PCR analysis of the expression of M-cell markers in conventional epithelia from the ileum and cecum of GST (control) or GST-RANKL injected mice. Results are normalized to *Gapdh* expression and are presented relative to the expression in ileal epithelium from GST-treated mice. Data are representative of two independent experiments (error bars indicate standard deviation). Scale bars: 20 μm (a) and 100 μm (d).

Figure 6

RelB activity is essential for M-cell differentiation

(**a**) Western blot analysis of NF-κB proteins in the ileal and cecal epithelium with sequential treatment with RANKL. Epithelia were dissected at indicated days of the sequential administration. Nuclear fractions were isolated, and the obtained samples were subsequently subjected to western blotting for indicated proteins in figures as described in *Methods*. Data are representative of two independent experiments. Optical densities were measured from scanned X-ray films and normalized to densities of lamin A/C (right panels). (**b**) Whole-mount immunohistochemical images of Tnfaip2 and GP2 in ileal epithelia of ALY/NscJcl-aly/aly (aly/aly) or ALY/NscJcl-aly/+ (aly/+) mice injected with GST or GST-RANKL. Administrations of GST or GST-RANKL were performed as described in *Methods.* The aly/+ mice were used as controls. The ileal specimen is composed of villi and many crypts. (**c**) Quantitative PCR analysis of the expression of M-cell markers. Results are normalized to *Gapdh* expression and are

presented relative to the expression in the ileal epithelium from GST-treated mice. Data are representative of four animals per group. Error bars indicate standard deviation. Scale bars: 50 μm (a).

Figure 7

Nuclear translocation of RelB disappearing from M cells on cecal FAE of C57BL/6 mice.

(**a** and **b**) Single confocal planes of the ileal (**a**) and the cecal FAE and crypt (**b**) of C57BL/6 mice. FAE monolayers were stained with anti-RelB, anti-Spi-B antibodies, phalloidin, and Hoechst 33342 as the indicated colors. F-actin staining visualizes cell borders by the detection of actin filaments. Arrowheads indicate examples of Spi-B-positive RelB-negative cells.

Scale bars: 20 μm (a).

Figure 8

Small numbers of M cells in the cecal FAE express nuclear RelB.

(**a**) Histograms of the fluorescence intensity of nuclear RelB in the ileal FAE and the cecal FAE of C57BL6/N mice. Nuclear fluorescence intensities were measured from images of whole-mount immunohistochemistry with an antibody against Spi-B and RelB as described in *Methods*. Black lines represent cells stained with the anti-RelB antibody, and gray lines represent cells stained without the anti-RelB antibody. (**b**) Scatter plots of the fluorescence intensities of RelB versus Spi-B. Over 8,000 cells

were counted from more than ten whole-mount images of FAE from three C57BL/6 mice. The numbers indicated in the scatter plots are the proportions of each boxed area to the whole cells. Data are representative of three independent experiments. (c) Scatter plots summarizing the proportions of RelB-positive cells in total FAE cells (left) or in total M cells (Spi-B-positive cells) (right). ***$P < .001$; P values were calculated by Dunnett's test.

Figure 1

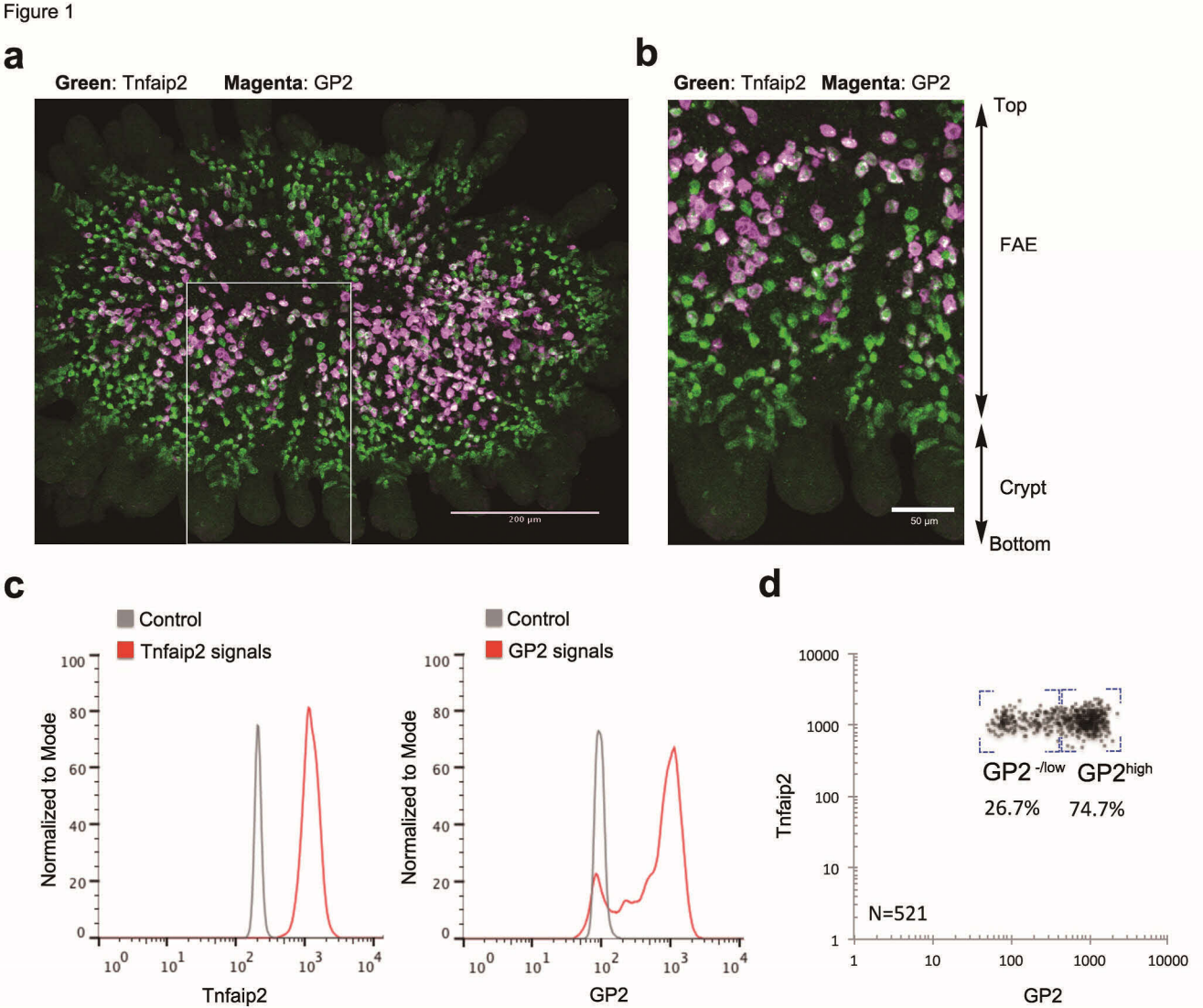
a
Green: Tnfaip2 Magenta: GP2
200 μm
b
Green: Tnfaip2 Magenta: GP2
Top
FAE
Crypt
Bottom
50 μm
c
Control
Tnfaip2 signals
Normalized to Mode
Tnfaip2
Control
GP2 signals
Normalized to Mode
GP2
d
Tnfaip2
GP2 -/low
GP2 high
26.7%
74.7%
N=521
GP2

Figure 2

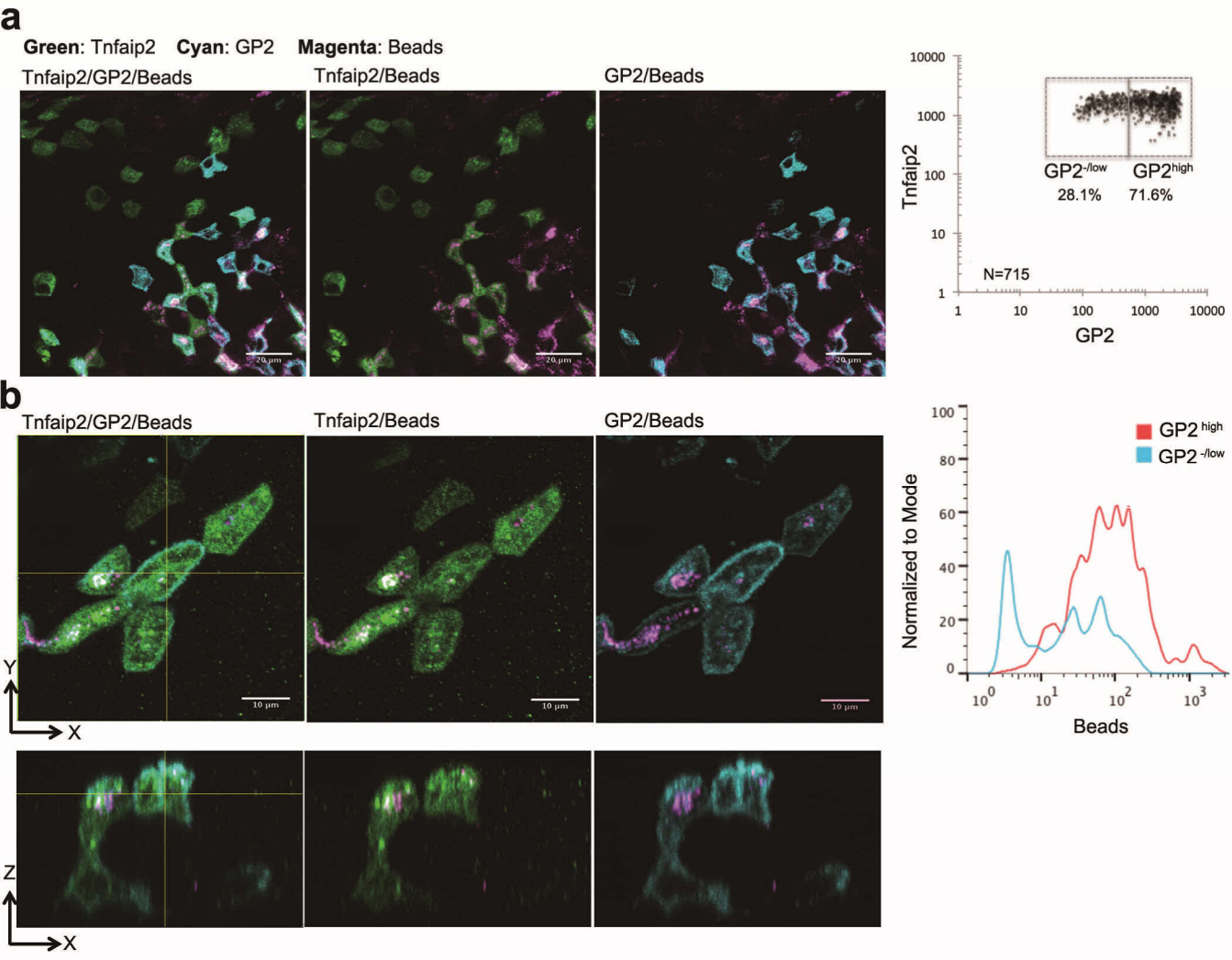
a
Green: Tnfaip2 Cyan: GP2 Magenta: Beads
Tnfaip2/GP2/Beads
Tnfaip2/Beads
GP2/Beads
20 μm
Tnfaip2
GP2
GP2-/low
GP2high
28.1%
71.6%
N=715
b
Tnfaip2/GP2/Beads
Tnfaip2/Beads
GP2/Beads
10 μm
Y
X
Z
X
Normalized to Mode
GP2 high
GP2 -/low
Beads

Figure 3

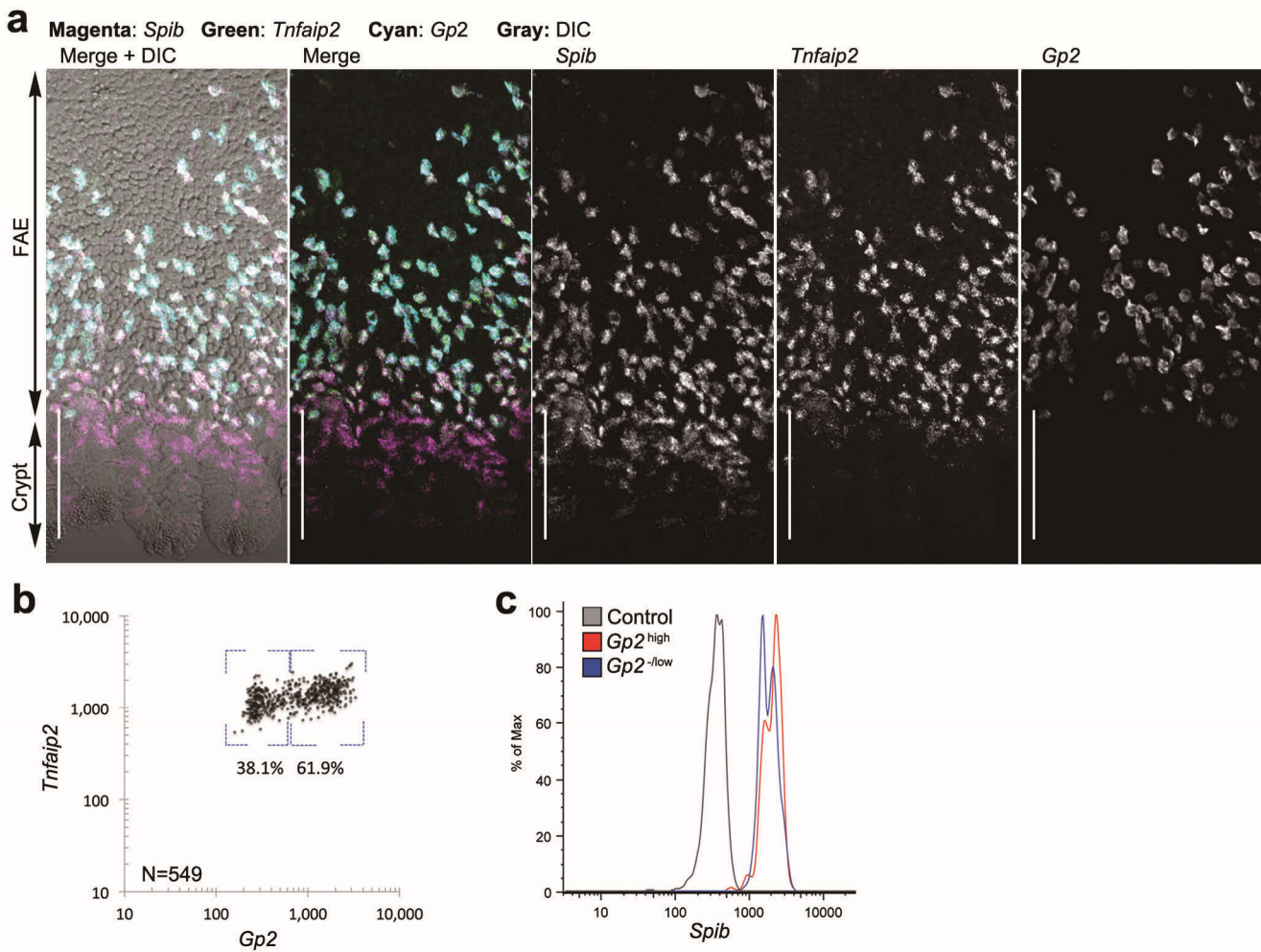
a
Magenta: Spib Green: Tnfaip2 Cyan: Gp2 Gray: DIC
Merge + DIC
Merge
Spib
Tnfaip2
Gp2
FAE
Crypt
b
10,000
1,000
100
10
Tnfaip2
38.1% 61.9%
N=549
10
100
1,000
10,000
Gp2
c
Control
Gp2 high
Gp2 -/low
100
80
60
40
20
0
% of Max
10
100
1000
10000
Spib

Figure 4

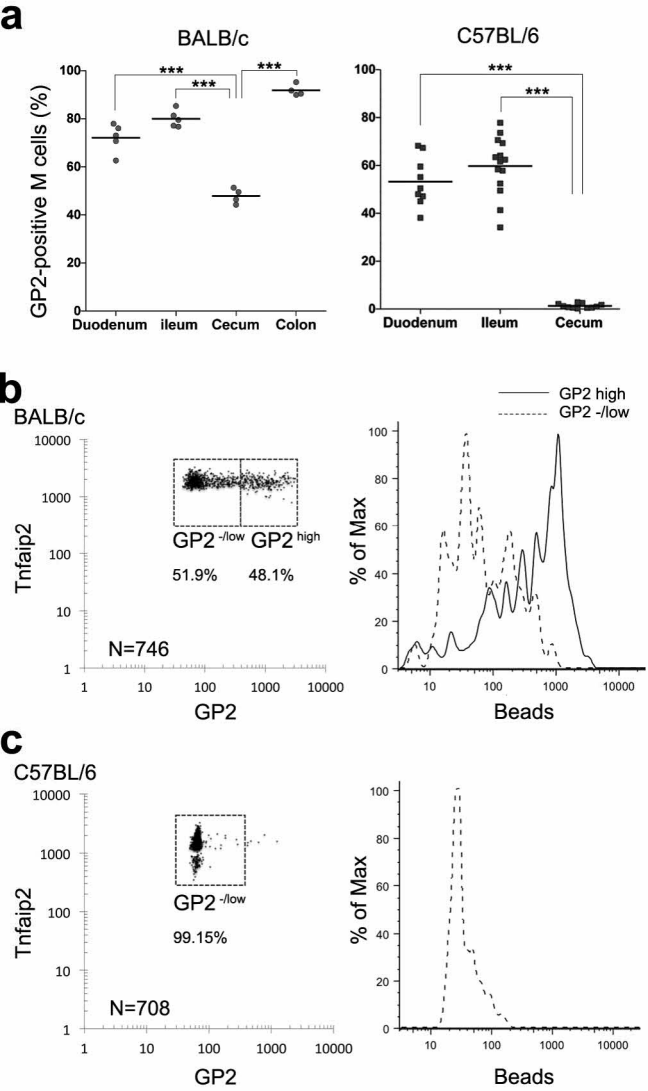
a
BALB/c
C57BL/6
GP2-positive M cells (%)
***
Duodenum
ileum
Cecum
Colon
Ileum
b
BALB/c
GP2 high
GP2 -/low
Tnfaip2
GP2 -/low
GP2 high
51.9%
48.1%
N=746
GP2
% of Max
Beads
c
C57BL/6
99.15%
N=708

Figure 5

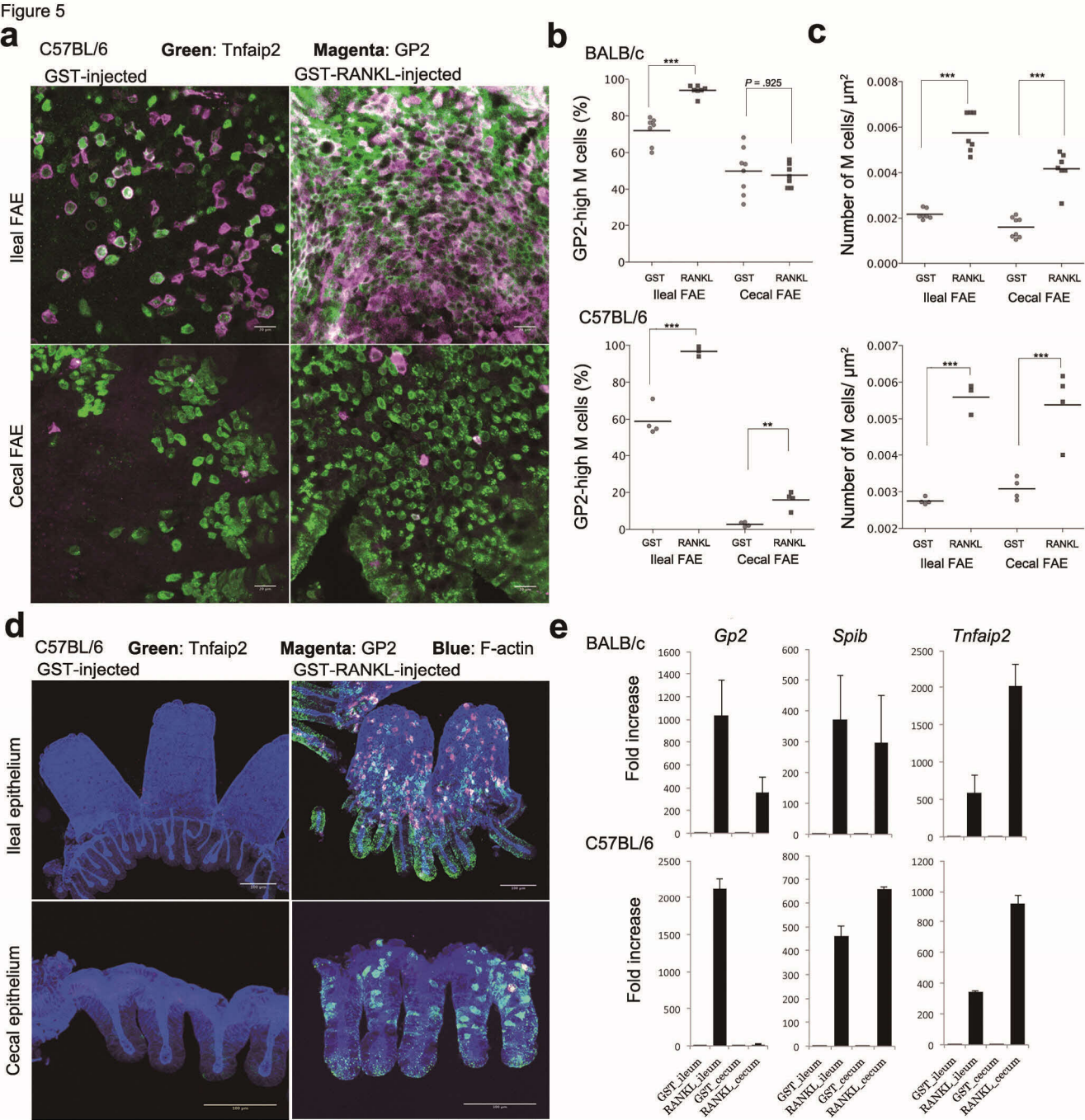
a
C57BL/6
Green: Tnfaip2
Magenta: GP2
GST-injected
GST-RANKL-injected
Ileal FAE
Cecal FAE
b
BALB/c
GP2-high M cells (%)
***
P = .925
GST
RANKL
Ileal FAE
Cecal FAE
C57BL/6
**
c
Number of M cells/ µm²
d
C57BL/6
Green: Tnfaip2
Magenta: GP2
Blue: F-actin
GST-injected
GST-RANKL-injected
Ileal epithelium
Cecal epithelium
e
BALB/c
Gp2
Spib
Tnfaip2
Fold increase
C57BL/6
GST_ileum
RANKL_ileum
GST_cecum
RANKL_cecum

Figure 6

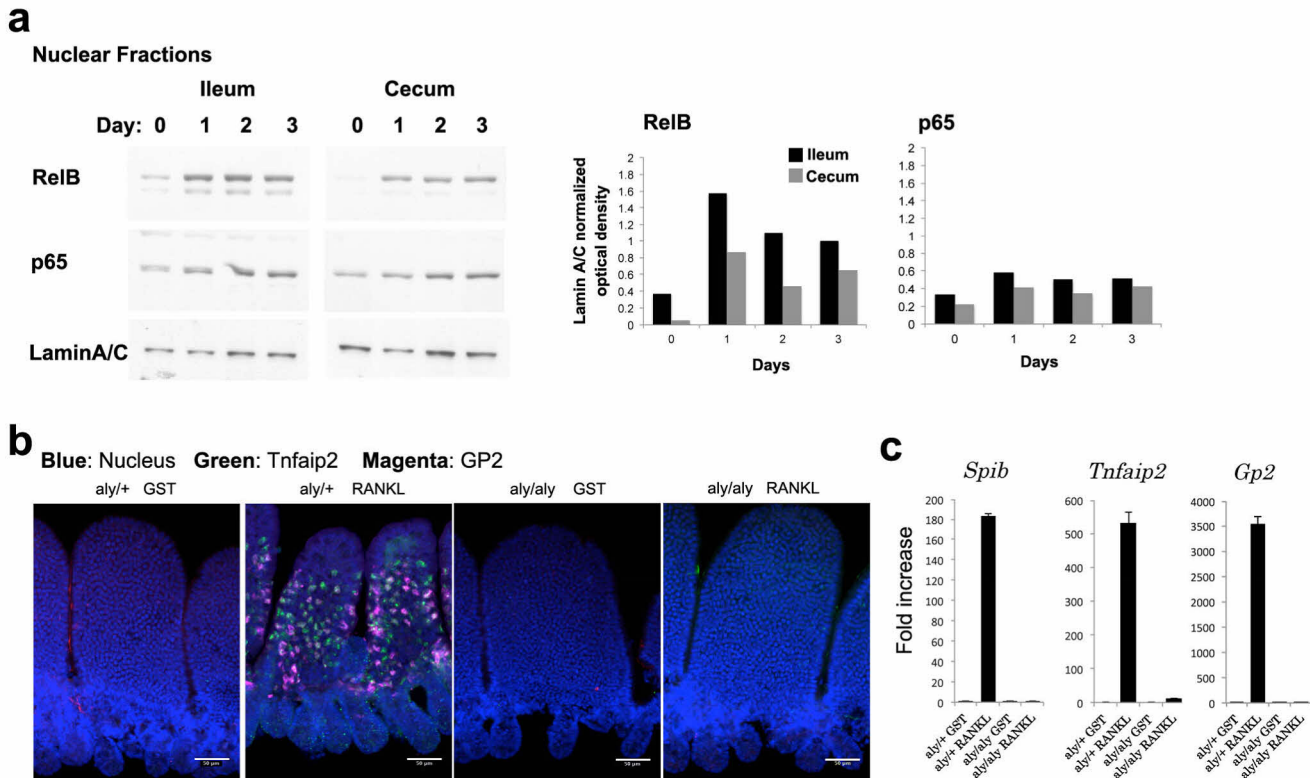
a
Nuclear Fractions
Ileum
Cecum
Day: 0 1 2 3 0 1 2 3
RelB
p65
LaminA/C
RelB
p65
Ileum
Cecum
Lamin A/C normalized optical density
Days
Days
b
Blue: Nucleus Green: Tnfaip2 Magenta: GP2
aly/+ GST
aly/+ RANKL
aly/aly GST
aly/aly RANKL
c
Spib
Tnfaip2
Gp2
Fold increase
aly/+ GST
aly/+ RANKL
aly/aly GST
aly/aly RANKL

Figure 7

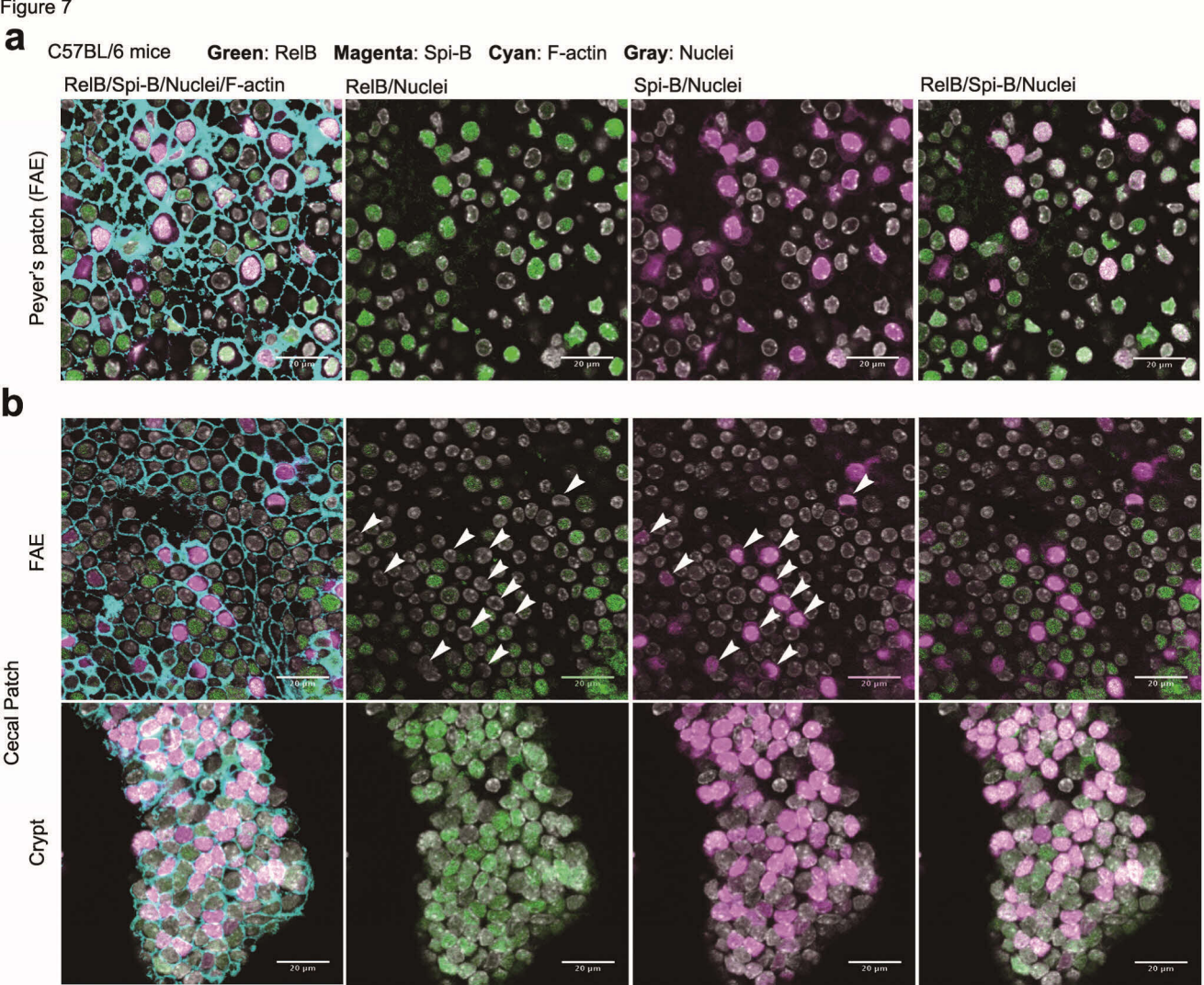
a
C57BL/6 mice
Green: RelB
Magenta: Spi-B
Cyan: F-actin
Gray: Nuclei
RelB/Spi-B/Nuclei/F-actin
RelB/Nuclei
Spi-B/Nuclei
RelB/Spi-B/Nuclei
Peyer's patch (FAE)
b
FAE
Cecal Patch
Crypt
20 μm

Figure 8

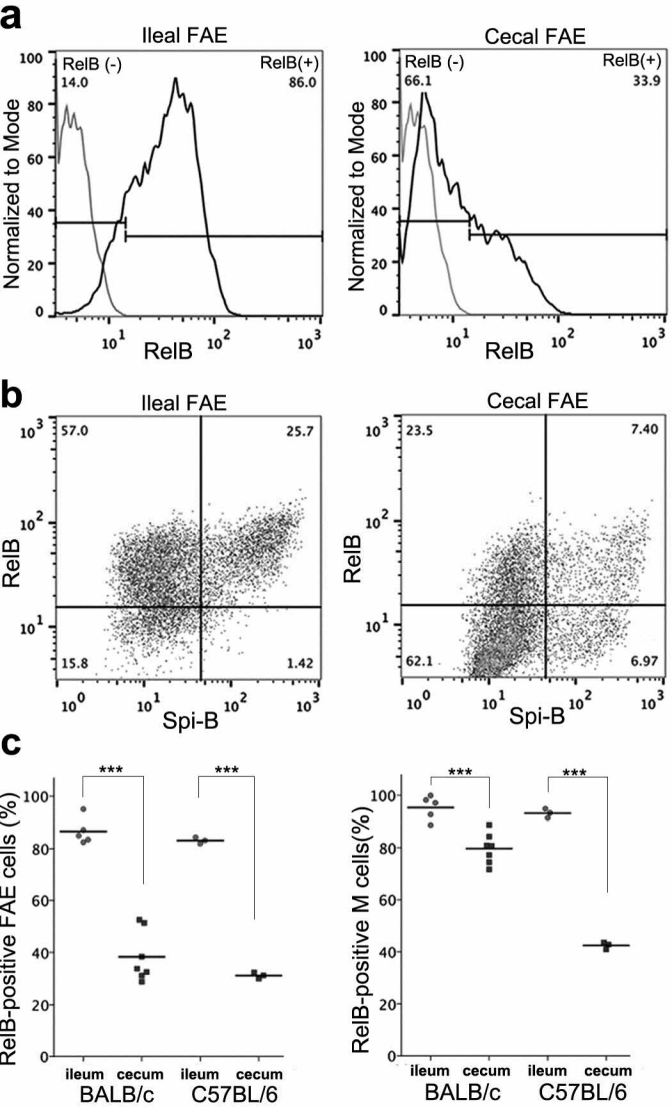
a
Ileal FAE
RelB (-)
14.0
RelB(+)
86.0
Normalized to Mode
RelB
Cecal FAE
RelB (-)
66.1
RelB(+)
33.9
Normalized to Mode
RelB
b
Ileal FAE
57.0
25.7
15.8
1.42
RelB
Spi-B
Cecal FAE
23.5
7.40
62.1
6.97
RelB
Spi-B
c
RelB-positive FAE cells (%)
***
***
ileum
cecum
ileum
cecum
BALB/c
C57BL/6
RelB-positive M cells(%)
***
***
ileum
cecum
ileum
cecum
BALB/c
C57BL/6

Supplemental information

Supplemental Figure Legends

Supplemental Figure 1

Preparation of the epithelial monolayer from murine Peyer's patches.

(**a**) A dissecting stereomicroscopic view showing the luminal side of a Peyer's patch of a BALB/c mouse. (**b**) A view from the serosal side of a FAE-containing epithelial sheet which was separated from the lamina propria by manipulation after treatment with EDTA as described in Materials & Methods. The translucent circles are FAEs, and the surrounding area is occupied by numerous crypts. (**c**) One FAE with associated crypts is isolated. (**d**) Immunohistochemistry on a cryosection of an obtained FAE monolayer using ZO-1 (Green), E-cadherin (Magenta) antibodies, and DAPI (Blue). Scale bars: 500 μm (a and b), 200 μm (c) and 20 μm (d).

Supplemental Figure 2

Morphological features of Tnfaip2-expressing cells fit with those of M cells.

The top portion (a and b) and the bottom portion (c and d) of the FAE dome are shown separately. (**a** and **c**) The left panels of each figure are images of the luminal surface of the FAE stained for F-actin and displayed as gray scale images. The right panels are same microscopic fields of left panels to show Tnfaip2 (Green) and GP2 (Magenta) expression. In contrast to the smooth staining of F-actin on surrounding enterocytes, the coarse staining of F-actin on the surface of Tnfaip2-expressing cells reveals irregular brush borders. (**b** and **d**) Slices images from consecutive confocal images along the a-b

line of the right panels in a and c. The cell nuclei were stained with Hoechst 33342 (Cyan). These sliced images also reveal basolateral pocket-like structures containing mononuclear cells. Scale bars: 20 μm.

Supplemental Figure 3

Immunoelectron microscopic analysis for Tnfaip2 in FAE of Peyer's patch

Immunoreactivity of Tnfaip2 was detected predominantly in the cytoplasm of M cells which lack microvilli on their apical surface. Capital M shows M cell. Scale baer: 1 μm.

Supplemental Figure 4

Reactivity to UEA-I lectin in Tnfaip2-expressing cells.

(**a**) Whole-mount immunohistochemistry of the FAE monolayer and surrounding crypts for Tnfaip2, GP2, and UEA-I. Each of the indicated channels is shown separately in a gray scale. UEA-I detects M cells on the FAE but also labels Paneth cells at the bottom of crypts surrounding FAE as described previously.[17] (**b**) Scatter plot of the fluorescence intensities of Tnfaip2 versus GP2. (**c**) Histograms of the fluorescence intensity of UEA-I in GP2-low or GP2-high M cells within the indicated boxed areas of the scatter plot. The blue and red lines represent GP2-low and GP2-high cells, respectively. A gray line represents a control experiment performed without UEA-I. Scale bars: 100 μm (a).

Supplemental Figure 5

Sequential expression of three markers during M cell differentiation

Colocalization of M cells and migrating EdU–positive cells. (a) FAE of mice which were injected with EdU as indicated time before the mice were killed were subjected to whole-mount immunohistochemistry using Spi-B antibody. (b) The proportion of colocalization of each M-cell markers with EdU signal was measured by Image J software. Scale bars: 100μm.

Supplemental Figure 6

Spi-B is expressed continuously during the entire process of M-cell differentiation.

Whole-mount immunohistochemical image of the FAE stained for Spi-B, Tnfaip2, and GP2 as indicated by colors. Each of the indicated channels is shown separately in a gray scale. Scale bars: 100 μm.

Supplemental Figure 7

Another three signature genes of the M cell during their maturation process.

FISH images stained with oligonucleotide probes for *Pglyrp1* (a), *Anxa5* (b), or *Ccl9* (c) are compared with *Spib* and *Gp2*. *Pglyrp1, Anxa5, and Ccl9* all show almost identical expression patterns with *Spib*. Each indicated channel is shown separately in a gray scale. Scale bars: 100 μm.

Supplemental Figure 8

A confocal image of whole-mount immunostaining using anti-Tnfaip2 (Green), GP2 (Magenta) and RANK (Blue) antibodies. The left panel is the cecal FAE of BALB/c,

and the right panel is that of C57BL/6 mice. (**c**) Three color FISH images of the cecal FAE of a C57BL/6 mouse for *Spib*, *Tnfaip2*, and *Gp2* are shown in the gray scale. Scale bars: 200 μm (b) and 100 μm (c).

Supplemental Figure 9

Comparable distribution of CCL20 and RANKL-RANK in Peyer's patches and the cecal patches from C57BL/6 mice.

(**a**) Three-color whole-mount immunostaining of the ileal FAE (upper panels) and the cecal FAE (lower panels) by using anti-CCL20, Tnfaip2, and GP2 antibodies. Each channel is shown separately in a gray scale. (**b**) Immunohistochemistry of tissue sections from the ileal Peyer's patch and the cecal patch by using anti-RANKL and RANK antibodies. Cell nuclei were stained with TOPRO-3. Scale bars: 200 μm.

81 Supplemental Table1

82 Antibodies and a lcetin used for immunohistochemistry

Antigen	Source	Catalog No.	Dilution (IHC)	Dilution (WB)
CCL20	R&D systems	AF760	1:200	
E-cadherin	R&D systems	AF748	1:200	
GP2	MBL	D278-3	1:400	
RANK	R&D systems	AF462	1:200	
RANKL	ebioscience	14-5952	1:100	
RelB	Santa Cruz Biotechnology	SC-226	1:100	1:2000
Spi-B	R&D systems	AF7204	1:200	
Tnfaip2	House made		1:200	
UEA-I lectin	Vector Laboratories	RL-1062	1:400	
ZO-1	Life Technologies	61-7300	1:100	
p65	Santa Cruz Biotechnology	SC-372		1:2000
LaminA/C	GeneTex	GTX1116777		1:2000

83

Supplemental Table 2

List of the oligonucleotide primers used for quantitative PCR

Target gene (Accession No.)	Forward	Reverse
Gp2 (NM_025989)	5'-GATACTGCACAGACCCCTCCA-3'	5'-GCAGTTCCGGTCATTGAGGTA-3'
Tnfaip2 (NM_009396)	5'-GTGCAGAACCTCTACCCCAATG-3'	5'-TGGAGAATGTCGATGGCCA-3'
Spib (NM_019866)	5'-CCGAGGGGAGGGGATCTGAG-3'	5'-GGAGGAGAACTGGAAGACGCCG-3'
Gapdh (NM_008084)	5'-TGTGTCCGTCGTGGATCTGA-3'	5'-TTGCTGTTGAAGTCGCAGGAG-3'

Supplemental Table 3

Effect of environment condition on the populations of GP2-positive M cells

BALB/c	Peyer's patches	Cecal patches
Conventional [3]	79.98 ± 3.51 (5)	47.85 ± 3.16 (4)
Germ Free [3]	79.49 ± 9.96 (4)	39.53 ± 6.76 (3)

C57BL/6	Peyer's patches	Cecal patches
Conventional [6]	59.73 ± 12.19 (14)	1.28 ± 0.90 (11)
Germ Free [3]	53.70 ± 9.53 (9)	1.20 ± 1.06 (11)

FAEs prepared from mice housed under the indicated conditions [number of mice]. Values give mean ± S.D. (number of FAE samples).

Supplemental Figure 1

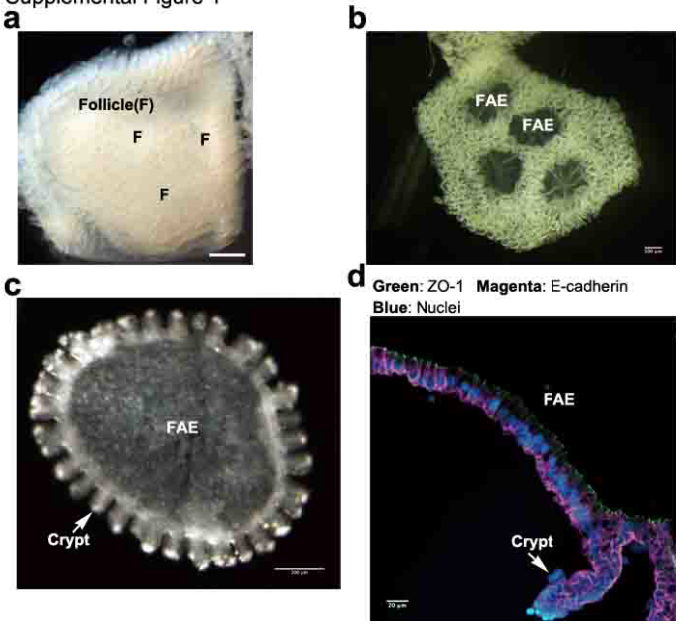

Supplemental Figure 2

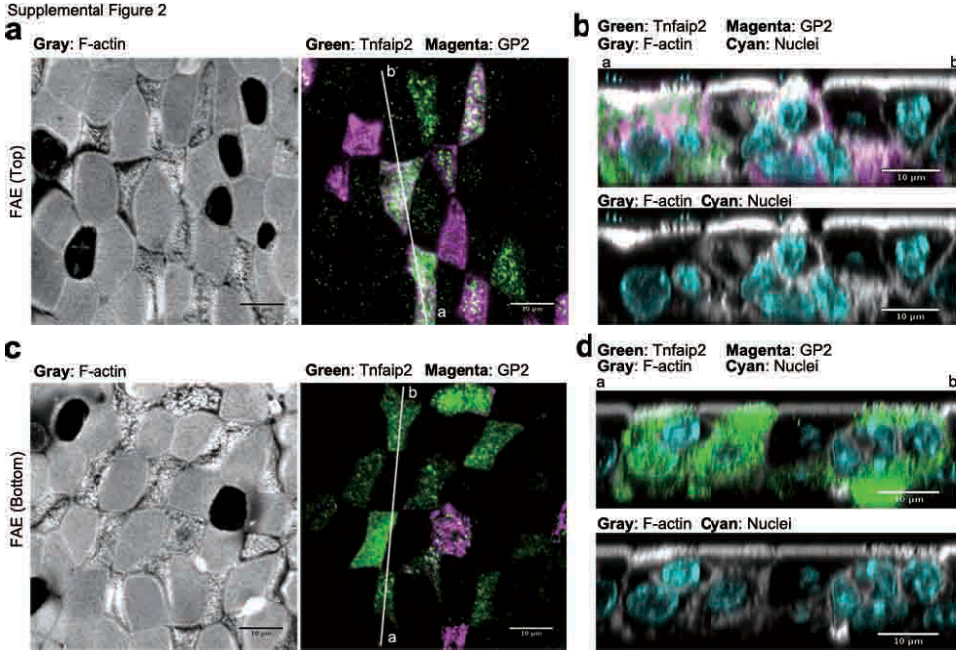

Supplemental Figure 3

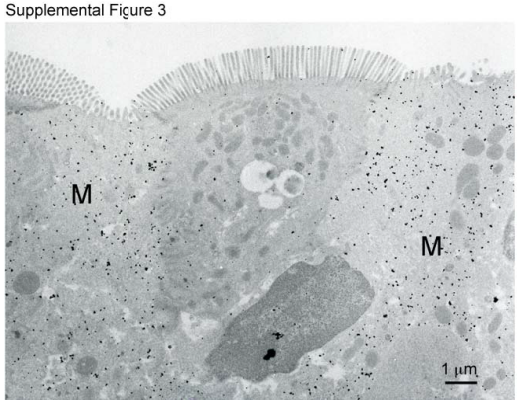

Supplemental Figure 4

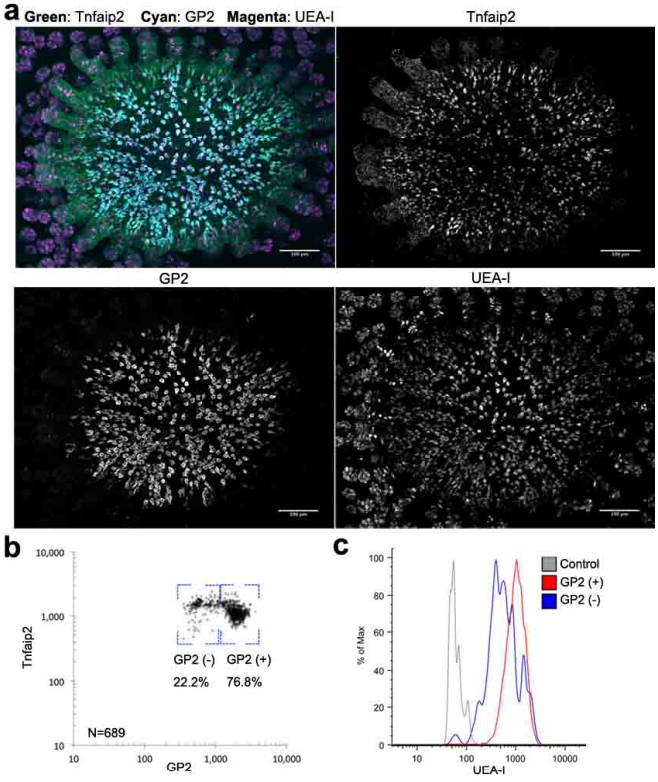

Supplemental Figure 5

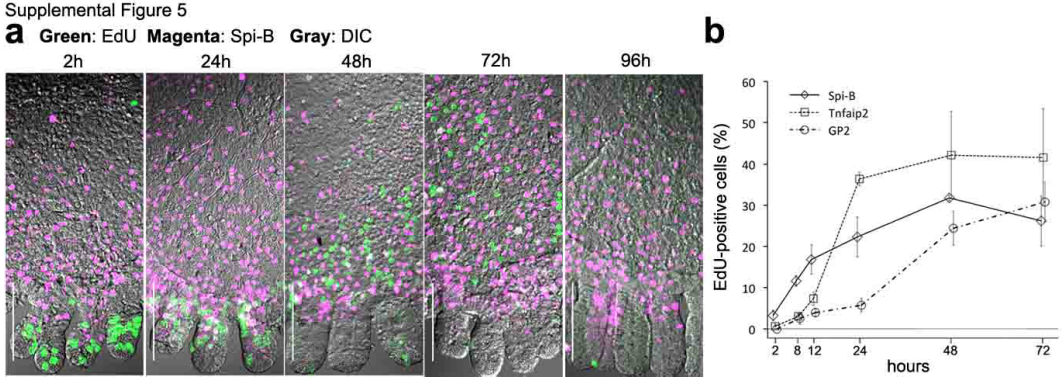

Supplemental Figure 6

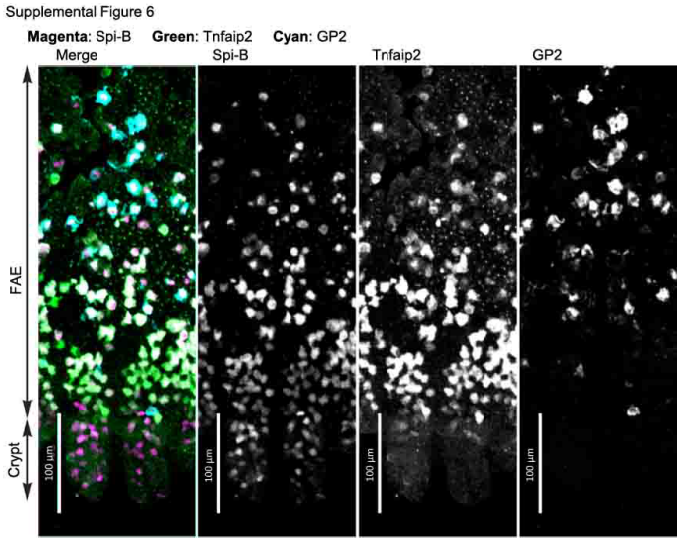

Supplemental Figure 7

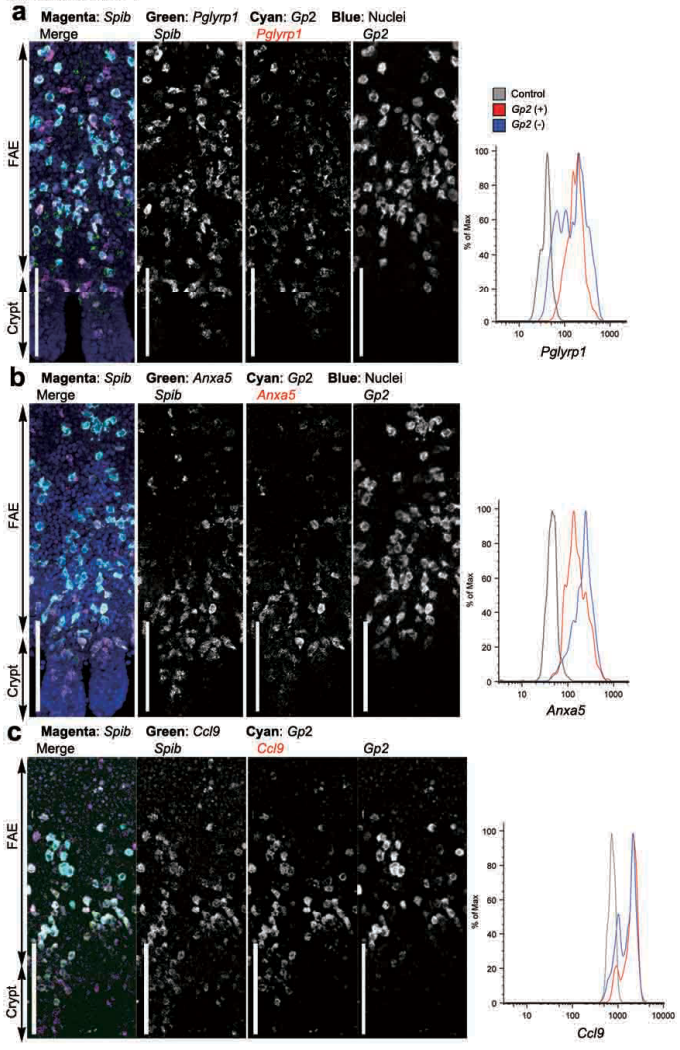

Supplemental Figure 8

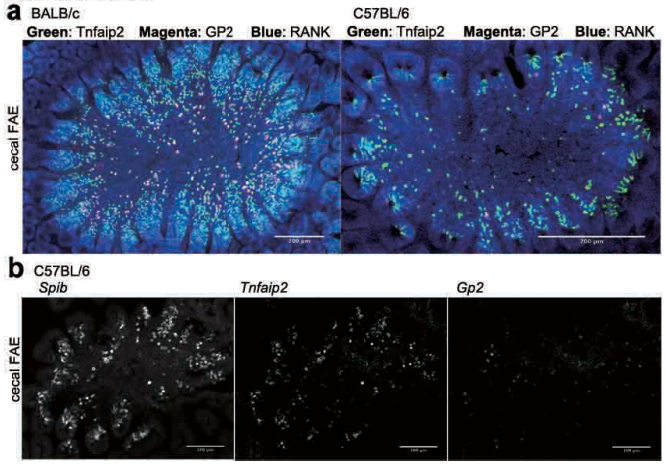
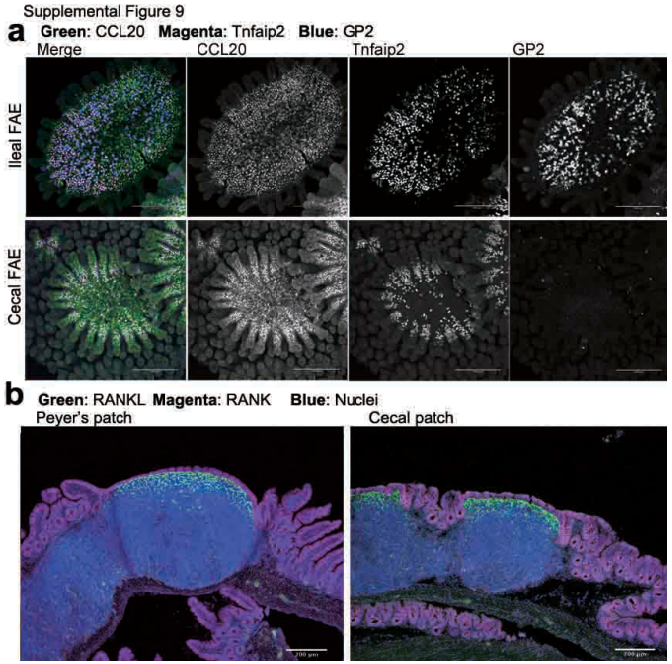
Supplemental Figure 9